Cooling Concepts for High Power Density Magnetic Devices

J. Biela and J. W. Kolar
Power Electronic Systems Laboratory, ETH Zurich
ETH-Zentrum, ETL H23, Physikstrasse 3
CH-8092 Zurich, Switzerland
Email: biela@lem.ee.ethz.ch

***Abstract*— In the area or power electronics there is a general trend to higher power densities. In order to increase the power density the systems must be designed optimally concerning topology, semiconductor selection, etc. and the volume of the components must be decreased. The decreasing volume comes along with a reduced surface for cooling. Consequently, new cooling methods are required. In the paper an indirect air cooling system for magnetic devices which combines the transformer with a heat sink and a heat transfer component is presented. Moreover, an analytic approach for calculating the temperature distribution is derived and validated by measurements. Based on these equations a transformer with an indirect air cooling system is designed for a 10kW telecom power supply.**

***Index Terms*— Transformer, Inductor, Heat Pipe, Thermal Management.**

I. Introduction

In the area of power electronic converter systems there is a general trend to higher power densities which is driven by cost reduction, an increased functionality and in some applications by the limited weight/space (e.g. automotive, aircraft). In order to reduce the volume of a system, first the most appropriate topology for the intended application must be chosen.

In the next step the parameters of the system/topology – like switching frequency, number of turns, values of the components etc. – must be optimised so that the overall converter size is minimised. Additionally, some of the passive components could be integrated in order to reduce the volume further [1], [2].

Based on the analytic model and optimisation procedure presented in [3] these steps have been accomplished in [4] for a series-parallel resonant converter for process technology/telecom applications. There, an increase of power density by a factor of approximately 3-5 compared to modern state-of-the-art power supplies has been achieved. Furthermore, the dependency of the power density on various system parameters, like max. junction temperature, control dynamic, cooling system, has been examined. Based these optimisations three conclusions can be drawn:

- The optimal switching frequency in terms of power density for the resonant converters/considered application is in the range of 100. . .200kHz. Increasing the switching frequency leads to a larger overall volume since the volume increase of the cooling system outweighs the relatively small volume reduction of the passive components.
- For a high power density a high heat sink temperature and a good thermal coupling between the semiconductors and especially the passive components and the heat sink is mandatory.
- In compact systems a relatively large share of the volume (up to 50%) is required for mounting the components since the housings do not match each other geometrically and for the air flow since the components are cooled via their surfaces.

The latter issue could also be seen in the photo of the telecom power supply shown in figure 2 whose schematic is given in 1 [5]. The transformer of this supply will be used as a practical example for the following considerations. The power density of the supply is 760W/dm^3 (13W/in^3) and for cooling the passive components – especially the transformers – additional fans and volume for the flowing air are provided.

For increasing the power density of supplies the space between the components and for the air flow must be re-

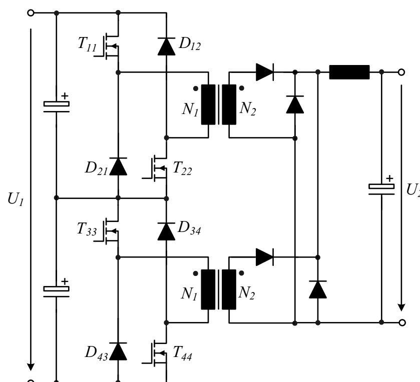

Fig. 1: Schematic of the telecom power supply.

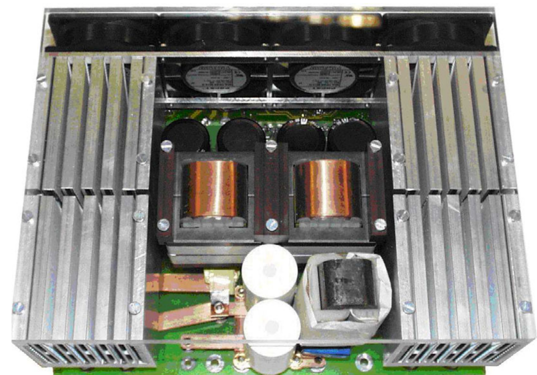

Fig. 2: Picture of the telecom power supply.

	Free Convection	Forced Air Cooling	Indirect Forced Air Cooling (HTC)
$\frac{S_{Cooling}}{V_{Trans.}}[m^{-1}]$	40-80		100-400 500-900 (HS only)
$\alpha_{Surface}\left[\frac{W}{m^2K}\right]$	5-15	30-60	300-600
Power Density $[kW/dm^3]$	-	5-15	20-50 (..-100 Xfrm only)

TABLE I: Key figures for different cooling methods where $S_{Cooling}/V_{Trans.}$ is the ratio of the cooled surface to the volume of the magnetic device, $\alpha_{Surface}$ specifies the heat transfer coefficient, HS stands for heat sink and Xfrm denotes a transformer.

Switching frequency	25kHz
Input voltage	800V +/-3%, DC
Input current	13.3A
Output voltage	48-56V
Output current	208A@48V, 180A@56V
Output power	10 kW
Efficiency (at rated power)	94.0%
Maximum ambient temp.	40°C
Length	270mm (10.6in)
Width	320mm (12.6in)
Height	170mm (6.7in)

TABLE II: Specification of the telecom power supply in figure 2.

duced. Also the volume of the components must be lowered. With a decreasing volume, however, also the surface of the components, which is especially in magnetic devices used for dissipating the heat, is decreasing if the aspect ratio is approximately constant. Consequently, the losses which could be removed via the surface of the component are decreasing for an increasing power density since the heat transfer coefficient of the surface $\alpha_{Surface}$ is limited for forced air cooling (cf. table I).

Since for a fixed voltage and current level the overall losses in the magnetic devices usually do not significantly drop with an increasing frequency/decreasing volume due to high frequency losses the ratio power loss per surface area is rising when the power density is increased. This would lead to higher temperatures in the magnetic device since the amount of heat which could be dissipated via a fixed surface is limited for a fixed temperature and air velocity [6].

In order to keep the temperatures below the maximum value the heat transfer coefficient of the surface and/or the surface itself must be increased. This could be achieved by combining a transformer with an additional heat sink. There, the heat of the transformer is not dissipated directly via the surface of the magnetic devices to the air but via a heat sink which enables a much more efficient cooling with respect to volume usage. With this method the heat transfer coefficient increases by a factor of 5-10 and the surface per volume ratio by 2-10 referring to standard forced air cooling (cf. table I).

In the following Section II first the original design of the transformer for the considered telecom supply and the data of the new transformers with heat transfer component (HTC) are presented together with the principal construction of the HTC and appropriate materials for the HTC. In order to be able to calculate the temperature distribution in the transformer/HTC and to compare different setups an analytical thermal model of the transformer/HTC is derived in Section III. Thereafter, the model is validated by measurements and temperature distributions for different HTC materials are calculated and compared with the original design of the transformer in Section IV. Since the HTC usually is made of highly electrical (thermal) conductive materials and is placed close to the magnetic core the eddy currents and the related losses in the HTC are calculated in Section V. Finally, a conclusion is presented in Section VI.

II. Thermal coupling of transformer and heat sink

The concept of the direct thermal coupling is examined on the basis of the transformers used in the telecom power supply shown in figure 2 but could be applied to any magnetic device. The specification of the supply is given in table II. Both transformers are forced air cooled and each made of two E70 cores in parallel and a foil winding with a turns ratio of 18:3. Under full load the winding temperature rises up to approximately 129°C ($T_{Ambient} = 40°C$).

With a forced air cooling system the heat is dissipated via the surface of the transformer. The thermal resistance between the surface and the ambient could be calculated by

$$R_{th} = \frac{1}{\alpha_S S_T}, \tag{1}$$

where S_T is the exposed surface and α_S is the heat coefficient of the surface. This coefficient could be estimated by

$$\begin{aligned} \alpha_S &= \frac{k}{L}\, 0.102\, Re_D^{0.675}\, Pr^{1/3} \\ &\approx \frac{3.33 + 4.8v^{0.8}}{L^{0.288}} \end{aligned} \tag{2}$$

with

$$\begin{aligned} Re_D &= \frac{vL}{\nu} \quad \text{Reynolds-number} \\ L &= \text{Characteristic length in [m]} \\ v &= \text{Air Speed in [m/s]} \\ \nu &= \text{Kinetic viscosity of air} \\ Pr &= \text{Prandtl-number} \\ k &= \text{Thermal conductivity of the air,} \end{aligned}$$

which is based on empirical calculations and experimental results published in [8], [7].

For the considered telecom supply a thermal resistance between the transformer surface and the ambient of approximately 1.7 $[\frac{K}{W}]$ results which corresponds well with the measured temperatures.

The low value of the thermal resistance is mainly due to the relatively large surface of the transformer ($\approx$220 cm^2) and the high velocity of the flowing air ($\approx$3 $[\frac{m}{s}]$). However, due to the cubic transformer shape the large surface area comes along

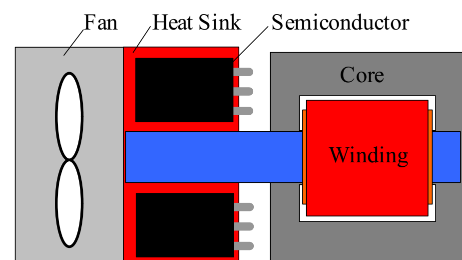

Fig. 3: Possible construction of the thermal connection between a heat sink and a transformer.

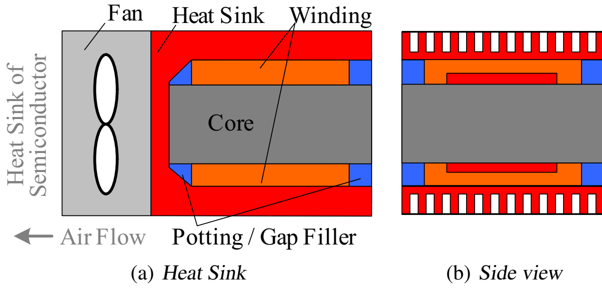

(a) *Heat Sink* (b) *Side view*

Fig. 4: (a) Transformer with special heat sink. (b) Side view of the heat sink including transformer.

with a large volume (296 cm^3) and a low ratio of surface per volume of 74.5 [m^{-1}] (cf. table I).

For increasing the surface/volume ratio planar cores (e.g. ELP) might be considered, which have a larger core surface area. With the high output current of the considered power supply, however, most of the losses are generated in the winding and a large share of the losses must be dissipated through the core (yokes) if planar cores are used. This would result in a comparatively large temperature drop across the core [13]. Furthermore, the winding length increases for planar cores compared to standard/cubic core shapes what results in higher overall losses and a lower efficiency of the transformer.

As described above, another problem in principle is, that the surface area decreases with increasing power density and/or decreasing volume of the transformer.

Instead of dissipating the losses via the surface of the transformer a heat sink (e.g. the heat sink of the semiconductors) could be used which has a surface/volume ratio in the range of 700...1000 [m^{-1}] [11]. For coupling the transformer thermally to the heat sink either a heat transfer component (HTC - cf. fig. 3) could be used or the transformer is directly mounted on / connected to the heat sink – for example via some potting material or via a pad. In case the transformer is mounted directly on the heat sink the relatively large footprint requires a large area on the base plate what results in a larger heat sink volume.

This could be avoided if a special heat sink for the transformer is designed. A possible construction is shown in figure 4. There, it is possible to put the heat sink on the intake side of the fan and the heat sink of the semiconductors on the outlet side. Since the power loss of the transformer usually is much smaller than the losses in the semiconductors the temperature of the cooling air for the semiconductors heat sink is only slightly increased compared to ambient temperature.

However, the design of a special heat sink for the transformer is quite complex, cost-intensive and dependant on the transformer design. Consequently, only the coupling methods via a HTC (e.g. fig. 3) and more standard heat sinks are considered in the following.

A. Design of the new transformers

In table III the parameters of the original transformer with two parallel connected E70 cores and of two new transformers are given. All three transformers have 18 primary and 3 secondary turns.

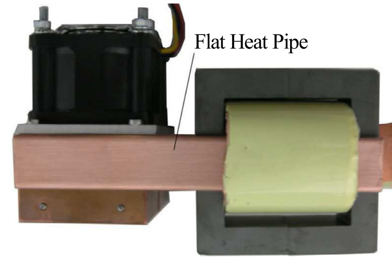

Fig. 5: Photo of the measurement setup with a heat transfer component using a heat pipe.

The original transformer is designed so that it reaches its maximum allowed operation temperature and the maximum possible flux density including a safety margin under full load conditions. Therefore, the switching frequency must be increased for the two new transformers in order to avoid saturation since the core area is decreased with the volume. Increasing the number of primary turns is not a reasonable alternative since this would lead to higher winding losses, which are already relatively high in the original design.

As could be seen in table III the ratio losses per surface P/S increases with decreasing transformer volume although the surface per volume ratio S/V also increases for the smaller cores and the losses of the E55/21 core are smaller than the losses of the original design due to an interleaving of the primary and secondary. Consequently, the maximum temperature rise increases and the two smaller transformers can not be operated continuously under full load with the original cooling system. Therefore, a HTC cooling system for the smaller E55/21 is examined in the following.

	f_S [kHz]	P_P [W]	P_S [W]	P_C [W]	P_Σ [W]	$\frac{S}{V}$ [m^{-1}]	$\frac{P}{S}$ [W/m^2]
2×E70	25	11.9	29.0	6.0	46.9	74.5	2.1
E65	60	11.5	28.0	8.7	48.3	119	3.5
E55/21	75	9.2	22.1	7.9	39.3	149	4.1

TABLE III: Parameters of the transformers for the telecom supply (P_P/P_S Losses in the primary/secondary winding, P_C core losses and P_Σ overall losses).

B. Materials for the HTC

For the HTC a material with a high thermal conductivity is required. This could be a copper bar with a thermal conductivity of $\lambda = 380$ [W/K/m], a bar made of industrial diamonds in an aluminium matrix with $\lambda \approx 650$ [W/K/m] [9] or a heat pipe with $\lambda > 10000$ [W/K/m] as shown in figure 5.

In order to reduce the thermal resistance of the HTC also several paths could be connected in parallel – for example one on the upper and one on bottom side of the transformer/heat sink as shown in figure 12. In the following the temperature distribution in a cooling system with a HTC as shown in figure 3 is calculated in order to compare different setups analytically.

III. Thermal Model

The thermal behaviour of the HTC and the thermal interfaces to the heat sink, the core and the winding could be modelled by the equivalent circuit given in figure 6 which is based on the design shown in figure 3. In the model the interface between the HTC and the heat sink on the left hand side (blue box) is represented by an distributed thermal

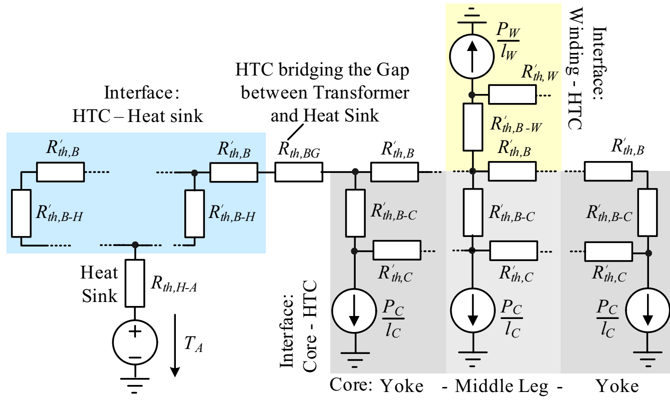

Fig. 6: Distributed thermal model of the cooling system shown in figure 3 with the heat sink on the left hand side, a gap between heat sink and transformer and the transformer with winding on the right hand side.

network with thermal resistances per unit length. The thermal conductivity between the HTC and the heat sink is described by $R^{'}_{th,B-H}$ and the conductivity of the HTC itself by $R^{'}_{th,B}$. The temperature distribution in this area could be calculated by using transmission line equations (lossy lines without energy storage) what results in the following differential equation ($0 < x \leq l_{HS}$):

$$\frac{\mathrm{d}^2 P_{HTC}(x)}{\mathrm{d}x^2} = P_{HTC}(x)\frac{R^{'}_{th,B}}{R^{'}_{th,B-H}} \qquad (3)$$

$$T_{HTC}(x) = -\int_0^x P_{HTC}(\tilde{x})R^{'}_{th,B}d\tilde{x} + T_{HS}$$

with the inital conditions

$$P_{HTC}(0) = 0$$

$$P_{HTC}(l_{HS}) = -(P_C + P_W)$$

and with

$$P_{HTC}(x) = \text{Power through HTC at } x\ [W]$$
$$R_{th,H-A} = \text{Thermal R of heat sink } [K/W]$$
$$R^{'}_{th,B-H} = \text{Thermal R: HTC – heat sink } [K/W/m]$$
$$R^{'}_{th,B} = \text{Thermal R of HTC } [K/W/m]$$
$$T_{HS} = \text{Temperature heat sink } [^\circ C]$$
$$T_{HTC} = \text{Temperature HTC } [^\circ C]$$
$$l_{HS} = \text{Length: HTC-heat sink interface } [m]$$
$$P_C = \text{Losses in the core } [W]$$
$$P_W = \text{Losses in the windings } [W].$$

In this approach it is assumed that the heat is only dissipated via the heat sink and that the base plate of the heat sink is approximately isothermal due to its high thermal conductivity. With the solution of the differential equation the temperature distribution in the HTC could be calculated by

$$T_{HTC}(x) = \frac{(P_C+P_W)\sqrt{R^{'}_{th,B}R^{'}_{th,B-H}}\cosh\frac{\sqrt{R^{'}_{th,B}}x}{\sqrt{R^{'}_{th,B-H}}}}{\sinh\frac{\sqrt{R^{'}_{th,B}}l_{HS}}{\sqrt{R^{'}_{th,B-H}}}}.$$

Between the heat sink and the transformer is a small gap which could be used for interconnecting the semiconductors mounted on the heat sink and for the outlet of the air. This gap could be omitted for the sake of an increased thermal coupling due to a reduced length of the HTC and a direct thermal coupling of the core to the heat sink in case the transformer is neither at the outlet nor the intake side of the fan and the space is not needed for interconnections.

In the gap the temperature distribution in the HTC is given by ($l_{HS} < x \leq l_{HS} + l_G$):

$$P_{HTC} = P_C + P_W \qquad (4)$$

$$T_{HTC} = R^{'}_{th,B}\frac{x-l_{HS}}{l_{HS}}(P_C+P_W) + T_{HTC}(l_{HS})$$

with

$$l_G = \text{Length of gap } [m],$$

what results in a linear temperature gradient.

On the outer parts of the transformer the HTC is only coupled to the yoke of the core. There, the heat flux could be calculated by solving the following ODE: ($l_{HS}+l_G < x \leq l_{HS}+l_G+l_{C,Y}$ and $l_{HS}+l_G+l_C-l_{C,Y} < x \leq l_{HS}+l_G+l_C$):

$$\frac{\mathrm{d}^3}{\mathrm{d}x^3}P_{HTC}(x) = \frac{(R^{'}_{th,B}+R^{'}_{th,C})}{R^{'}_{th,B-C}}\frac{\mathrm{d}}{\mathrm{d}x}P_{HTC}(x) - \frac{R^{'}_{th,C}}{R^{'}_{th,B-C}}\frac{P_C}{l_C} \qquad (5)$$

$$T_{HTC} = -\int_0^x P_{HTC}R^{'}_{th,B} + T_{HTC}(l_0)$$

with the ICS (cf. fig. 7):
($l_{HS}+l_G < x \leq l_{HS}+l_G+l_{C,Y}$):

$$P_{HTC}(l_0) = -(P_C + P_W)$$
$$P_{Cq}(l_0) = 0$$

($l_{HS}+l_G+l_C-l_{C,Y} < x \leq l_{HS}+l_G+l_C$):

$$P_{HTC}(l_0) = 0$$
$$P_{Cq}(l_0) = 0$$
$$\frac{\mathrm{d}^2}{\mathrm{d}x^2}P_{HTC}(l_0) = 0$$

and with

$$R^{'}_{th,B-C} = \text{Thermal R: HTC – core } [K/W/m]$$
$$R^{'}_{th,C} = \text{Thermal R of core } [K/W]$$
$$l_{C,Y} = \text{Length: HTC-yoke interface } [m]$$
$$l_C = \text{Length: HTC-core interface } [m]$$
$$l_W = \text{Length: HTC-winding interface } [m]$$
$$l_0 = l_{HS} + l_G \text{ or } l_{HS}+l_G+l_C-l_{C,Y},$$

where x must be shifted by $l_{HS}+l_G$ for the left and by $l_{HS}+l_G+l_C-l_{C,Y}$ for the right yoke. The initial conditions at the border between the yoke and the middle leg where the winding is located are dependent on the differential equation for the middle leg. Thus, the constants for the solutions of the

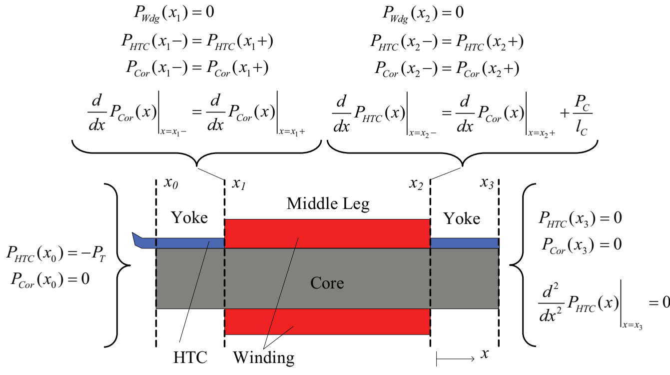

Fig. 7: Initial conditions/constraints for the differential equations of the temperature distribution in the HTC.

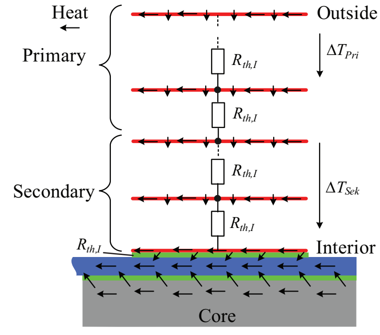

Fig. 8: Heat flow in the winding from the single layers to the HTC via the insulation ($R_{th,I}$).

differential equations in the three areas: yoke-leg-yoke must be calculated together.

In the middle leg heat is transferred to the HTC by the core at the bottom side and by the winding at the top side. The resulting equations are ($l_{HS}+l_G+l_{C,Y} < x \leq l_{HS}+l_G+l_C-l_{C,Y}$):

$$\frac{\mathrm{d}^2}{\mathrm{d}x^2}P_{HTC}(x) = P_{HTC}(x)\left(\frac{R'_{th,B}}{R'_{th,B-C}} + \frac{R'_{th,B}}{R'_{th,B-W}}\right) + P_{Cq}\frac{R'_{th,C}}{R'_{th,B-C}} + P_{Wq}\frac{R'_{th,W}}{R'_{th,B-W}} \quad (6)$$

$$\frac{\mathrm{d}}{\mathrm{d}x}P_{HTC}(x) = \frac{\mathrm{d}}{\mathrm{d}x}P_{Cq}(x) + \frac{\mathrm{d}P_{Wq}(x)}{\mathrm{d}x} + \frac{P_C}{l_C} + \frac{P_W}{l_W}$$

$$\frac{\mathrm{d}^2 P_{Cq}(x)}{\mathrm{d}x^2} = \frac{P_{HTC}R'_{th,B} + P_{Cq}R'_{th,C}}{R'_{th,B-C}}$$

$$T_{HTC} = -\int_0^x P_{HTC}R'_{th,B} + T_{HTC}(l_1)$$

with the ICS:
($l_{HS}+l_G+l_{C,Y} < x \leq l_{HS}+l_G+l_C-l_{C,Y}$):

$$P_{Wq}(l_1) = 0$$
$$P_{Wq}(l_2) = 0$$
$$P_{HTC}(l_\nu-) = P_{HTC}(l_\nu+)$$
$$P_{Cq}(l_\nu-) = P_{Cq}(l_\nu+)$$
$$\frac{\mathrm{d}}{\mathrm{d}x}P_{Cq}(x)\bigg|_{x=l_1-} = \frac{\mathrm{d}}{\mathrm{d}x}P_{Cq}(x)\bigg|_{x=l_1+}$$
$$\frac{\mathrm{d}}{\mathrm{d}x}P_{HTC}(x)\bigg|_{x=l_2-} = \frac{\mathrm{d}}{\mathrm{d}x}P_{Cq}(x)\bigg|_{x=l_2+} + \frac{P_C}{l_C}$$

and with

$$R'_{th,B-W} = \text{Thermal R: HTC – winding } [K/W/m]$$
$$R'_{th,W} = \text{Thermal R of winding } [K/W]$$
$$l_1 = l_{HS}+l_G+l_{C,Y}$$
$$l_2 = l_{HS}+l_G+l_C-l_{C,Y}.$$

For calculating the temperature distribution within the HTC and the transformer, first the differential equations for the two yokes and the middle leg must be solved. In the second step the 13 unknown constants in the solutions must be calculated by applying the initial conditions/constraints given in the equations 5 and 6 (cf. fig. 7).

A. Temperature drop across winding/core

So far only the temperature drop from the heat sink to the thermal interface of the winding and the core has been considered. The temperature drop within the winding and the core has been neglected and is calculated in the following.

In a foil winding the heat generated in the single layers flows from one layer via the insulation to the next layer until it reaches the interface: winding-HTC if in the worst case it is assumed that all losses are dissipated via the HTC and the heat sink.

The temperature drop within the copper layers is very small compared to the drop in the insulation. Therefore, it is neglected in the following. Furthermore, it is assumed that a thermally conductive adhesive tape like BondPly^{TM} [10] is used for insulating the layers (cf. $R_{th,I}$ in 8). This reduces the thermal resistance between the layers significantly. Based on the mentioned assumptions the temperature drop ΔT_{Wdg} across the winding could be calculated by [4]

$$\Delta T_{Wdg} = \Delta T_{Pri} + \Delta T_{Sec} = R_{th,I}\left(\sum_{\nu=1}^{N_{Pri}}\frac{\nu P_{Pri}}{N_{Pri}} + \sum_{\nu=1}^{N_{Sec}}\left(\frac{\nu P_{Sec}}{N_{Sec}} + P_{Pri}\right)\right)$$

with

$$R_{th,I} = \frac{d_I}{\alpha_I l_{Wdg} l_W}[K/W]$$
$$P_{Pri} = \text{Losses in primary winding } [W]$$
$$P_{Sec} = \text{Losses in secondary winding } [W]$$
$$N_{Pri}/N_{sec} = \text{Number of primary/secondary turns,}$$

where α_I is the thermal conductivity and d_I the thickness of the insulation layer. There, the thermal conductivity of the winding in the direction of the copper layers is much higher than the conductivity across the insulation, i.e. the equivalent circuit for the winding has an anisotropic thermal conductivity.

For the parameters of the E55/21 core in the telecom supply and BondPly^{TM} as insulation a worst case maximum temperature drop of 19.1°C results in the winding if no heat is dissipated via the surface of the winding. The real value is lower since a share of the losses is also dissipated via the surface.

The temperature drop in the core is given by

$$\Delta T_{Core} = \frac{R_{th,Leg}}{2}P_{Leg} \quad (7)$$

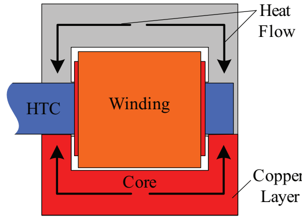

Fig. 9: Heat flow in the magnetic core - improved by copper layer.

with

$$R_{th,Leg} = \text{Thermal resistance of the core leg}[K/W]$$
$$P_{Leg} = \text{Heat generated in the heat flow path,}$$

where the heat flow path starts in the middle of the outer leg (where the two E-core halves are joint together) and runs through the yoke to the middle leg/HTC. Due to the relatively low thermal conductivity of ferrite the drop in the core could be high (25°C for the E55/21) if is assumed that no heat is dissipated via the surface. In order to reduce the temperature drop across the core thin (1mm) copper foils are bonded on the top side of the core where also the HTC is located (cf. fig. 9). This reduces the temperature drop to 5.4°C which could be calculated by

$$\Delta T_{Core,CU} = \frac{\sqrt{R'_{th,Leg} R'_{th,CU}}}{\tanh \frac{R_{thCU'}}{R'_{th,Leg}}} P_{Leg} \tag{8}$$

with

$$R'_{th,Leg} = \text{Per unit thermal R of the core leg}[K/W]$$
$$R'_{th,CU} = \text{Per unit thermal R of the copper layer}[K/W],$$

resulting from the mentioned transmission line approach for modelling the temperature distribution.

IV. Results for different HTCs

With the equations derived in the preceding sections the temperature distributions in transformers with HTC could be calculated. In order to validate the results a test setup as shown in fig. 10(a) has been built and the temperature distribution has been measured with thermocouples and an infrared camera (cf. fig.10(b)).

The heat was generated with a copper foil winding whose connectors were heated so that approximately no heat was dissipated via the connectors. Moreover, the transformer was put in a thermally isolated housing so that only a small amount of heat is dissipated directly via the transformer surface.

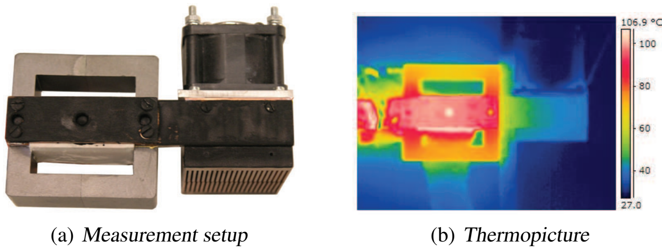

(a) *Measurement setup* (b) *Thermopicture*

Fig. 10: (a) Setup for temperature measurement with optimised copper heat sink [11] and (b) related measurement with thermo camera.

HTC	Size	T_{HTC}	T_W	Remark
Cu	3×17	102.7°C	115.6°C	
Cu	3×17	107°C	116°C	Measurement
H-P	3×17	50.6°C	61°C	$\lambda \approx 5000 K/W$
H-P	3×17	53°C	65°C	Measurement

TABLE IV: Calculated and measured temperatures for a copper HTC and a heat pipe.

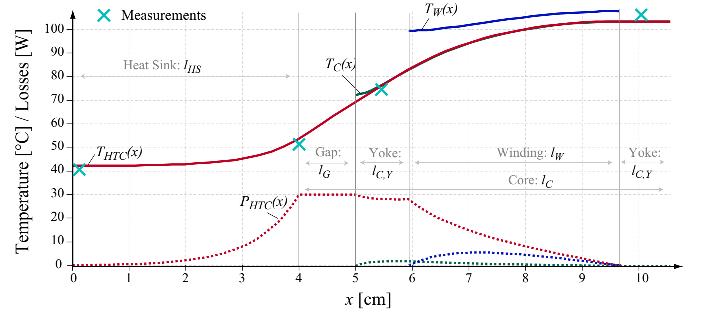

Fig. 11: Distribution of temperature and losses for a HTC made of copper for 40°C ambient temperature.

In table IV the resulting analytical and measured values for a HTC made of copper and of a heat pipe are given. There, the calculated values agree very well with the measured ones. This could be also seen in figure 11 where the calculated temperature/power flow distribution for the test setup with copper HTC is plotted.

With the validated equations the temperature distribution for different possible setups for the telecom power supply are calculated. The results for the E55/21 core with a 17mm wide HTC in different configurations are given in table V. There, the thickness of the HTCs is either constantly 3mm or 3mm in the region of the winding and 5mm outside this region.

For the calculations it has been assumed that the two transformers of the 10kW system are connected to the heat sink shown in figure 10(a) which has a thermal resistance of $R_{th,HS} = 0.31$ K/W, a volume of 0.12dm^3 and a cooling system performance index (CSPI) of 26.7 [W/K/dm^3]. The CSPI tells what cooling system power density could be achieved and is independent of system efficiency and temperature levels [11].

Due to the relatively high thermal resistance of the copper HTC the high temperature drop of 82K across the HTC results and causes a maximum winding interface temperature of $>$ 160°C. The temperature of the heat sink $T_{HS} = 64°C$ results with the total losses of app. 2×40W for both transformers and the thermal resistance of the heat sink. This temperature is independent of the HTC since it is always assumed that all

HTC	Size	T_{HTC}	T_W	T_C	$R_{th,HTC}$
Cu	3×17	146.0°C	149.6°C	146.4°C	2.65 K/W
2×Cu	3×17	107.1°C	109.4°C	107.5°C	1.67 K/W
2×Cu	3/5×17	101.2°C	103.5°C	101.6°C	1.53 K/W
Dia/Al	3×17	114.2°C	119.2°C	114.8°C	1.88 K/W
2×Dia/Al	3×17	90.1°C	92.9°C	90.4°C	1.25 K/W
Dia/Al	3/5×17	107.2°C	112.1°C	107.8°C	1.69 K/W
H-P	3×17	75.3°C	82.3°C	75.7°C	0.88 K/W

TABLE V: Maximum temperatures in the thermal interfaces for HTCs made of copper, diamond in Al-matrix and heat pipe without temperature drop in the winding/core.

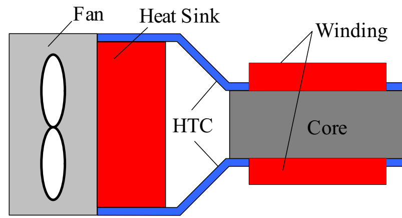

Fig. 12: Parallel connection of two HTCs for double sided cooling.

the losses are dissipated via the heat sink.

If two HTCs are connected in parallel as shown for example in figure 12 the thermal resistance between the transformer and the heat sink is halved. Therefore, the overall thermal resistance and the peak temperature of the transformer decreases significantly. This could be seen in row 1 and 2 of table V where the values for one and two parallel connected HTC are given.

A. Comparison

In the original transformer a maximum temperature of approximately 129°C was measured in the winding at full load. Taking the values given in table V and considering the temperature drop within the winding/core which are approximately 19°C (cf. preceding paragraph) an equal or even lower maximum temperature could be achieved either with two copper / diamond + AL-matrix HTCs in parallel or one HTC made of heat pipe. There, it is assumed as worst case that no heat is dissipated via the surface of the transformer.

With the heat pipe solution a relatively low thermal resistance could be achieved what results in an maximum possible output power of 6.5kW per transformer / 13kW for the converter and a maximum power density of 55kW/dm^3 for the transformer including heat sink.

In table VI the volume, the power density, the surface per volume and the efficiency for the transformer with E70 core and for the one with E55/21 core, HTC and heat sink are given. The power density of the new solution is more than 3 times higher than the power density of the 2×E70 transformer. By combining a transformer with a HTC and heat sink much more cooling surface per volume could be realised what results in a smaller possible overall volume for a given amount of losses. Due to the lower winding length and the reduced core volume also the efficiency is slightly increased.

In [12] and [13] planar cores with a power density of up to 109kW/dm^3 are published. The reasons for the high value are the lower power level and the relatively low current values. With an increasing power/current level the achievable power density reduces since the volume scales with m^3 and the surface only with m^2 so that the heat transfer deteriorates. This could also be seen in [14] where a 50kW transformer with a power density of 18kW/dm^3 is presented. There, and in the two other publications the additional volume of the heat sink, fan or convection which is required for cooling the transformer is not considered in the power density calculation. If only the transformer volume is considered a power density of 77.3kw/dm^3 results for the design with the E55 core.

	Vol [dm^3]	$\frac{P}{V}$ [kW/dm^3]	$\frac{S}{V}$ [$1/m$]	η
2×E70	0.29	13.1	74.5	99.0%
E55 + HTC + HS	0.118	42.3	365.9	
E55 + HP + HS (6.5kW)	0.118	55	365.9	99.0%

TABLE VI: Comparison between E70 and E55 transformer with HTC and heat sink (HS).

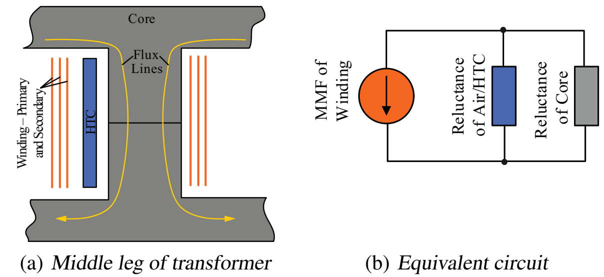

(a) *Middle leg of transformer* (b) *Equivalent circuit*

Fig. 13: (a) Middle leg of a transformer with a HTC in the window. (b) Simplified magnetic equivalent circuit of the Transformer.

V. Eddy Currents in the HTC

Since the HTC, made of thermally highly conductive material which are usually also very good electrical conductors, is placed close to the magnetic core/winding one has to consider also eddy currents/losses in the HTC which are induced by the AC magnetic fields. The losses, however, are relatively small since the magnetic field close to the ferrite core is quite small (usually some 100A/m for transformers in the kW range). The reason for this is the high permeability of the core and the low permeability ($\mu \sim 1$) of the air and the HTC - confer to fig. 13(a) where a section of the middle leg of a transformer is shown (the HTC is placed in the window). Due to the different permeabilities, the magnetic flux mainly flows through the core and not through the air and/or the HTC.

This could be also seen in the magnetic equivalent circuit which is shown on the right hand side of fig. 13(b). There, the winding is represented by a voltage source and the core and the air/HTC are modelled by magnetic reluctances/resistors. The current generated by the voltage source, which is equivalent to the magnetic flux, will mainly flow through the resistor with the lower resistance value (= magnetic core) as the magnetic flux does in the ferrite core.

In case the core would be removed, the path with high permeability/low magnetic reluctance is missing and the flux will mainly flow through the air/HTC. This would result in high eddy current losses in the HTC.

Since the run of the magnetic flux lines usually is 3 dimensional an accurate analytic calculation of the losses

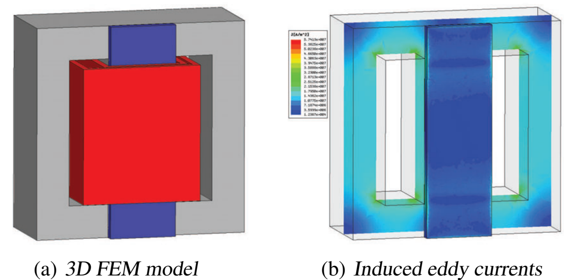

(a) *3D FEM model* (b) *Induced eddy currents*

Fig. 14: (a) 3D model used in the FEM-simulation. (b) Result of the FEM simulation with magnetic flux density in the core and current density in the HTC.

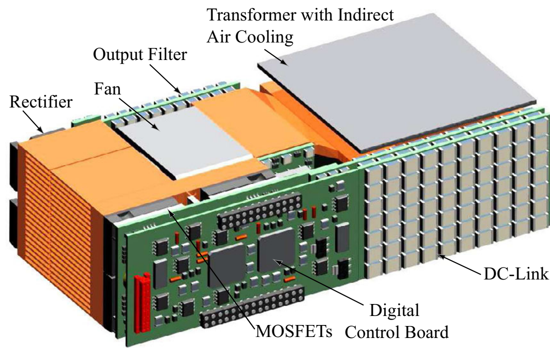

Fig. 15: Application of the indirect air cooling in a 5kW telecom power supply with 10kW/dm^3 and 1U height.

in the HTC is almost impossible and very time consuming. Based on some assumptions the field could be simplified to an 1D geometry (e.g. Dowell approach) and the losses can analytically approximated. The result for a transformer as used in the power supply ($\sim$1A magnetising current) is in the range of 10-20mW.

In case a FEM simulation of the set-up is performed also 3D effects for calculating the eddy currents can be considered. During a variety of simulations (cf. for example fig. 14 / 110mW losses in the HTC) it turned out that the additional losses in the HTC, including 3D-effects, are in the range of 50-150mW depending on the geometric arrangement of the components. Compared to the overall losses in the transformer of approximately 40W and the transferred power of 5kW these additional losses can be neglected.

So far only transformers have been considered. There, the air gap between the two halves of the E-cores is usually very small - ideally equal to zero. Thus, also the magnetic reluctance of the air gap and the fringing field of the gap are very small and can be neglected. In case of inductors either a core material with a low permeability (e.g. metal powder) or a core with a distinct air gap is used. There, the magnetic field close to the core/air gap is much larger than the field close to the ferrite core of the transformer. Consequently, the eddy current losses in the HTC will increase significantly.

On the other hand the eddy currents in the HTC attenuate the magnetic field outside the core/air gap. This reduces the losses in the inductor windings. The total losses, however, usually increase since the HTC is placed very close to the core/air gap. In order to limit the additional losses the HTC has to be designed in such a way that the eddy currents are limited - for example the distance between the HTC and the air gap could be increases by a recess.

VI. Conclusion

For increasing the power density of converter systems the volume of the magnetic components must be decreased amongst others. Since the component's efficiency usually is not increasing very much while reducing the volume the heat transfer to the ambient must be improved in order to limit the temperatures.

In this paper a cooling concept which couples a transformer with a heat sink by a heat transfer component made of copper, diamond + Al-matrix or a heat pipe is presented and compared with traditional forced air cooling systems. Based on this concept a transformer for a 5kW telecom power supply is redesigned what results in an three times increase of the power density of the transformer and an improved efficiency. With a HTC made of heat pipes a maximum power density of 55kW/dm^3 for the transformer with cooling system are achieved without cooling via the surface of the transformer.

Based on the indirect air cooling system a redesign of the telecom supply has been performed, where also the topology and the switching frequency have been optimised. There, a power density of 10kW/dm^3 and an overall height of 1U (40mm) could be achieved (cf. figure 15).

References

[1] J.T. Strydom, "*Electromagnetic Design of Integrated Resonator-Transformers*," Ph.D. Thesis, Rand Afrikaans University, South Africa, 2001.

[2] I.W. Hofsajer, "*On electromagnetic Integration in Hybrid Electronic Structures*," D. Eng. Thesis, Industrial and Electronics Research Group, Faculty of Engineering, Rand Afrikaans University, May 1998.

[3] J. Biela and J.W. Kolar, "*Analytic Design Method for (Integrated-) Transformers of Resonant Converters using Extended Fundamental Frequency Analysis*," Proceedings of the 5th International Power Electronics Conference (IPEC), Niigata, Japan, April 4 - 8, 2005.

[4] J. Biela, "*Optimierung des elektromagnetisch integrierten Serien-Parallel-Resonanzkonverters mit eingeprägtem Ausgangsstrom*," Ph.D. Thesis, Eidgenössische Technische Hochschule – ETH Zürich, Switzerland, 2006.

[5] J. Miniböck, J.W. Kolar and H. Ertl, "*Design and Experimental Analysis of a 10kW Dual 400V/48V Interleaved Two-Transistor DC/DC Forward Converter System Supplied by a VIENNA Rectifier I*," Proceedings of the 41st Power Conversion / Intellegent Motion / Power Quality Conference, Nuremberg, Germany, June 6 - 8 (2000).

[6] W.G. Odendaal und J.A. Ferreira, "*A Thermal Model for High-Frequency Magnetic Components*," IEEE Transactions on Industry Applications, Vol. 35, Issue 4, July-Aug, 1999, pp. 924-931.

[7] M. Jackob, "*Heat Transfer*," John Wiley & Sons, New York, London 1949.

[8] A. van den Bossche und V.C. Valchev, "*Inductors and Transformers for Power Electronics*," CRC Taylor & Francis Group, London, New York, 2005.

[9] U. Drofenik and J.W. Kolar, "*Analyzing the Theoretical Limits of Forced Air-Cooling by Employing Advanced Composite Materials with Thermal Conductivities >400W/mK*," Proceedings of the 4th International Conference on Integrated Power Systems (CIPS'06), Naples, Italy, June 7 - 9, 2006.

[10] http://www.bergquistcompany.com

[11] U. Drofenik, G. Laimer und J.W. Kolar, "*Theoretical Converter Power Density Limits for Forced Convection Cooling*," Proceedings of the International PCIM Europe 2005 Conference, Nuremberg, Germany, June 7-9, pp. 608-619.

[12] W.A. Roshen, R.L. Steigerwald, R.J. Charles, W.G. Earls, G.S. Claydon and C.F. Saj, C.F., "*High-Efficiency, High-Density MHz Magnetic Components for Low Profile Converters*," IEEE Transactions on Industry Applications, Vol. 31, Issue 4, July-Aug., 1995, pp. 869-878.

[13] W.G. Odendaal, J. Azevedo, G.W. Bruning and R.M. Wolf, "*A High-Efficiency Magnetic Component with Superior Caloric Performance for Low-Profile High-Density Power Conversion*," IEEE Transactions on Industry Applications, Vol. 40, Issue 5, Sept.-Oct. 2004, pp. 1287-1293.

[14] M. Pavlovsky, S.W.H. de Haan and J.A. Ferreira, "*Design for better Thermal Management in High-Power High-Frequency Transformers*," Conference Record of the Industry Applications Conference, 2005, 40th IAS Annual Meeting, Vol. 4, 2-6 Oct, pp. 2615-2621.